ChemComm

Accepted Manuscript

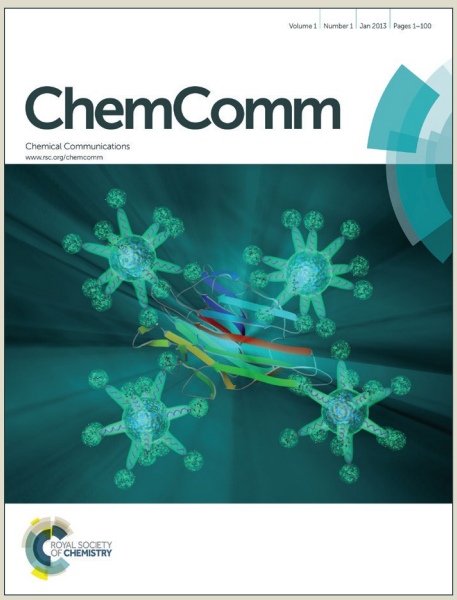

ROYAL SOCIETY OF CHEMISTRY

www.rsc.org/chemcomm

Journal Name

COMMUNICATION

Water oxidation catalysed by a mononuclear Co^{II} polypyridine complex; possible reaction intermediates and the role of the chloride ligand

Received 00th January 20xx,
Accepted 00th January 20xx

DOI: 10.1039/x0xx00000x

www.rsc.org/

Biswanath Das, Andreas Orthaber, Sascha Ott*, and Anders Thapper*

A mononuclear cobalt(II) complex as a homogeneous molecular catalyst for photochemically, electrochemically and chemically induced oxygen evolution reactions is presented. Experimental evidence points towards the presence of a chloride ligand at the cobalt centre throughout the catalytic cycle, and the temporary detachment of a pyridine ligand to open a coordination site for substrate binding.

The increasing problems associated with non-renewable energy sources have encouraged researchers to look for methods that can convert sunlight, an abundant energy source, to a chemical fuel. This could for example be achieved by splitting water to hydrogen and oxygen. The oxidative part of water splitting involves a four electron, four proton processes (eqn 1). In nature it is the Mn_4Ca core of the oxygen evolving centre in PSII that does this formidable job, using sunlight as the only energy input.[1]

$$2H_2O \longrightarrow 4H^+ + O_2 + 4e^- \quad (1)$$

The blue dimer, a diruthenium(III) complex $[(bpy)_2(OH_2)Ru^{III}–O–Ru^{III}(OH_2)(bpy)_2]^{4+}$, reported by Meyer et al. in 1982 opened up the field of small molecular units as water oxidation catalysts.[2] Thereafter, a large number of ruthenium and iridium complexes have been reported that show in some cases very promising water oxidation capabilities.[3] It is now well established that even mononuclear ruthenium and iridium complexes with robust ligand environment can act as catalysts for water oxidation.[3f-i]

While important catalysis principles can be studied in these catalysts, their large scale use is precluded because of the scarce nature of these noble metal complexes. In contrast, catalysts based on first row transition metals could be implemented in large scale applications as they are cheap, nontoxic and earth abundant. In this respect cobalt complexes have attracted attention, and a handful of them have been reported as water oxidation catalysts. These include molecular mononuclear complexes,[4] dinuclear complexes,[5] Co_4O_4 cubanes,[6] and tetracobalt polyoxometallates.[7] In order to arrive at a stable and efficient catalyst it is essential to find a robust ligand system that can hold the metal centre firmly and does not undergo self-oxidation in the oxidizing environment.[4a] Moreover, there must be at least one labile ligand at the metal to allow for substrate water binding.[4a] Polypyridyl ligands have the potential to be used in this respect, but there are only a few examples of Co^{II} polypyridyl complexes reported to catalyse water oxidation thus far.[4a,4c,5] On the basis of pH dependent electrochemical studies of the mononuclear Co^{II} complex $\{[Co^{II}(Py5)(OH_2)](ClO_4)_2\}$ (Py5 = 2,6-bis(methoxydi(pyridin-2-yl)methyl)pyridine) in the pH range 7.6-10, Wasylenko et al. have demonstrated that the complex acts as an electrocatalyst for water oxidation and proposed a possible pathway for oxygen evolution where the O-O bond forms through nucleophilic attack by an incoming water/hydroxide substrate on a Co^{IV}-hydroxy/oxo species to give a Co^{IV}–peroxide complex.[4a] Very recently, Crandell et al. have presented theoretical studies on the catalytic cycle of water oxidation catalysed by the same $\{[Co^{II}(Py5)(OH_2)](ClO_4)_2\}$ complex. The spin quartet Co^{IV}-oxyl complex has been proposed to be the catalytically most active species which undergoes nucleophilic attack by a hydroxide ion on the oxyl moiety to form a Co^{II}-peroxy intermediate, followed by oxygen evolution.[8]

Scheme 1. Synthesis of $[Co^{II}(Py5OH)(Cl)](BF_4)$ (2).

Inspired by these results, we have chosen Py5OH (**1**) (Scheme 1) as a robust, polydentate ligand framework to coordinate the Co centre. In contrast to the Py5 ligand reported by Wasylenko et al, ligand **1** features free OH groups which can be used as a starting point for further functionalization e. g. by linking anchoring groups for surface immobilization. Herein, we present the synthesis and characterization of the Co^{II} complex of **1**, $[Co^{II}(\mathbf{1})Cl](BF_4)$ (**2**), isolated with a chloride as the sixth ligand (Figure S1). Complex **2** has been investigated in electrochemical, photochemical and chemical water oxidation and oxygen evolution reactions. A combination of ESI-MS, UV-Vis, and EPR (electron paramagnetic resonance) spectroscopy allows us to propose a possible oxygen evolution mechanism (Scheme 2) where the chloride ligand stays coordinated to the metal and the coordination of the Py5OH ligand adapts during catalysis to allow binding of the substrate.

Department of Chemistry-Ångström Laboratory, Uppsala University, P.O.Box 523, 75120 Uppsala, Sweden. E-mail: anders.thapper@kemi.uu.se
Electronic Supplementary Information (ESI) available: X-ray crystal structure and crystallographic data of **2**. MS, EPR, DLS, additional UV-Vis, O_2 evolution and electrochemistry data for **2**, $\mathbf{2}^{ox}$, **3**, $\mathbf{3}^{ox}$ and **4**. See DOI: 10.1039/c000000x/

The pentapyridylcarbinol ligand (**1**) was prepared by the reaction of 2-bromopyridine, 2,6-pyridine dicarboxylic acid chloride and n-butyl lithium following the procedure reported by Jonas et al.[9] The mononuclear cobalt(II) complex **2** was obtained as a brown precipitate by adding one equivalent of $Co(BF_4)_2$ to a methanol solution of **1**, followed by the addition of one equivalent NaCl (Scheme 1). The brown precipitate was dissolved in a 10:1 CH_3CN-toluene mixture and slow evaporation of the solvents over a period of seven days produced shining brown black crystals of **2** of X-ray diffraction quality. The X-ray crystal structure of **2** (Fig. S1 and Table S1) reveals that the Co^{II} ion is firmly held by the pentadentate ligand with a Co-N (central pyridine) distance of 2.12(1) Å whereas the average Co-N distance for the other pyridine moieties is 2.14(1) Å. The two hydroxyl groups of the ligand stay at a Co···O distance of more than 4.5 Å, presenting no plausible direct interaction with the metal centre. The sixth coordination site of the Co^{II} ion is occupied by a chloride ion with Co-Cl distance of 2.44(2) Å.

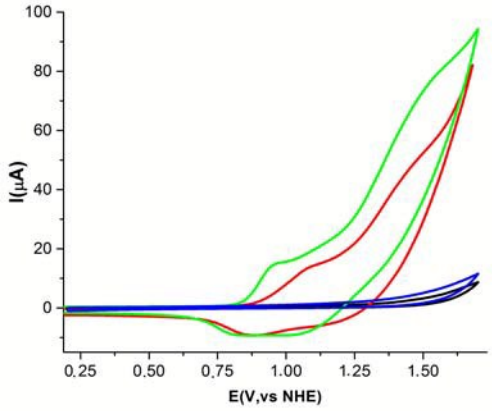

Fig. 1 Cyclic voltammetry of **2** (0.5 mM, pH 9 (green), pH 8 (red)) in 0.2 M borate buffer, and the buffers alone (pH 9 (blue), pH 8 (black)) at a scan rate of 50 mV s^{-1} under Ar atmosphere with a 3 mm glassy carbon working electrode, a glassy carbon rod counter electrode, and a Ag/AgCl (with saturated KCl aqueous solution) reference electrode.

The UV-Vis spectrum of a solution of complex **2** (0.5 mM) in a borate buffer (pH 8) shows a broad absorption shoulder at 485 nm (Fig. S2a). The EPR spectrum at 7 K shows an axial EPR signal with g values of 4.5 and 2.1 suggesting the presence of a high spin Co(II) centre (Fig. S3). The ESI-MS shows characteristic mass peaks at m/Z = 253.1 $([M^+–Cl^-]/2)^{2+}$, 505.1 $([M^+–Cl^-])$ and 541.1 $([M^+])$ in the positive detection mode (Fig. S4). These results show that **2** stays as a mononuclear complex in aqueous solution, and that the chloride ligand is not substituted by water.

The cyclic voltammetry of **2** in borate buffer (pH 8 and 9) is shown in Figure 1. A first quasi-reversible oxidation is found around 0.9V–1.0V (vs NHE), and is followed by a catalytic water oxidation wave at 1.2V-1.3V. This indicates that **2** can be effective as catalyst for water oxidation in the presence of photo-generated $[Ru(bpy)_3]^{3+}$ as oxidant (Eox = 1.3 V vs. NHE).[4c, 5a] The overpotential for water oxidation in the presence of **2** is 540 and 510 mV at pH 8 and 9, respectively,[†] very similar to that reported by Wasylenko et al. for $[Co(Py5)(OH_2)](ClO_4)_2$ at pH 9.2 (500 mV; 0.1 M phosphate buffer).[4a]

Light-driven water oxidation using **2** (0-10 μM) as catalyst was investigated in the borate buffer (pH 8) in the presence of $[Ru(bpy)_3]^{2+}$ as photosensitizer and $S_2O_8^{2-}$ as sacrificial electron acceptor.[10] Under illumination build-up of $[Ru^{III}(bpy)_3]^{3+}$ can be observed at 675 nm (Fig. S5), and photoproduction of oxidant is thus not limiting catalysis. Upon illumination oxygen evolution was observed with a turnover frequency (TOF) of 1.3±0.1 mol(O_2)mol(**2**)$^{-1}s^{-1}$ and a maximal turnover number (TON) of 51±1 mol(O_2)mol(**2**)$^{-1}$ (Fig. 2). The rate of oxygen evolution scales linearly with the concentration of **2** under the experimental condition (0–10 μM of **2**) (Fig. 2, inset).

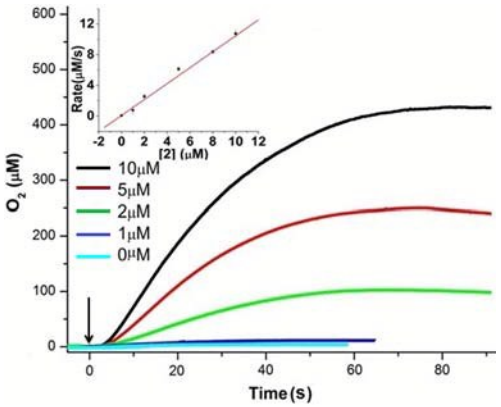

Fig. 2 Light-induced water oxidation in a solution (1 mL) containing **2** (0 μM, 2.0 μM, 5.0 μM, and 10.0 μM), $[Ru^{II}(bpy)_3](ClO_4)_2$ (0.15 mM), and $Na_2S_2O_8$ (3 mM) in borate buffer (0.1 M, pH 8). The Clark cell was kept constant at 20.1 °C, and the system was irradiated using LED (λ=470±10 nm, 820 μE cm^{-2} s^{-1}). The arrow indicates the start of the illumination. Inset: plot of oxygen evolution initial velocities (v) versus [**2**]. The rate, v, is calculated in the linear part of the oxygen evolution curves during the first 30 s of illumination.

Catalytic activity for water oxidation of **2** using chemical oxidation was also investigated. A freshly prepared aqueous solution of $[Ru(bpy)_3]^{3+}$ was added to a solution of **2** (2 μM) in borate buffer (pH 8) giving an initial Co to Ru^{III} molar ratio of 1:100 (Fig. S6a). A TON of 15±1 mol(O_2) mol(**2**)$^{-1}$ was observed, equivalent to a yield of ~60%. In a separate experiment a second addition of Ru^{III} triggered more oxygen evolution at a lower rate (Fig. S6b) demonstrating that the catalyst was still active at the end of the oxygen evolution.

The molecular integrity of **2** was investigated after oxidation with 10 eq of Ru^{III}. The addition of Ru^{III} led to oxygen evolution corresponding to ~1.5 mol(O_2) mol(**2**)$^{-1}$, i.e. a yield similar to when 100 eq Ru was used. Using ESI-MS we could detect peaks after the reaction corresponding to the presence of **2** (m/Z = 253, 505, and 541, Fig. S7). The integrity of the catalyst was also confirmed using dynamic light scattering (DLS) in borate buffer between pH 7.5–10, before and after illumination. No nanoparticle formation (1 nm–1000 nm) was observed in any of the samples prepared at pH <10. In contrast, at pH 10, the experiment after illumination showed distinct nanoparticle formation (of average hydrodynamic radius ~90nm) (Fig. S8).

Initial attempts to obtain further insights into intermediates that are involved in the catalytic cycle were conducted in borate buffer at pH 8. Addition of 5 eq of $[Ru^{III}(bpy)_3]^{3+}$ to **2** results in quantitative oxidation of the sample as evidenced by the disappearance of the Co^{II} signal in the EPR spectra at 7 K. Interestingly, the generated sample is EPR-silent (Fig. S3) which indicates the absence of any Co^{IV} species and the presence of a low spin Co^{III} complex as the dominating species under these conditions.

Since no oxidation states of the catalyst higher than +III could be observed in aqueous media, the oxidation of **2** was further studied in CH_3CN, i.e. a solvent that is not the substrate for the catalysis. Oxidations were performed using *m*-CPBA, a chemical oxidant which can also transfer an oxygen atom to the metal center. Although the pathway for water oxidation and oxygen evolu-

catalysed by **2** may be different in the two types of experiments, we argue that *m*-CPBA induced oxidation studies can be used to improve the understanding of key features in the catalytic cycle.

The EPR spectrum of **2** at 7 K in frozen CH_3CN shows an axial EPR signal very similar to that observed in borate buffer with g values of 4.5 and 2.1 (Fig. S9). ESI-MS of the CH_3CN solution shows the same mass peaks at m/Z = 253.1 ($[M^+-Cl^-]/2$), 505.1 ($[M^+-Cl^--H^+]$) and 541.1 ($[M^+]$) as in aqueous solution (Fig. S4b), confirming the integrity of **2** in CH_3CN. A cyclic voltammogram of **2** in CH_3CN shows two quasi reversible redox waves at 0.65 and 1.05 V vs. NHE corresponding to the Co(III)/Co(II)[11] and Co(IV)/Co(III) redox couples, respectively (Fig. S10).

Interestingly, the UV-Vis spectrum of the greenish-blue CH_3CN solution of **2** (0.5 mM) shows two distinct absorption bands with maxima at 588 (ε = 860 M^{-1} cm^{-1}) and 685 nm (ε = 1180 M^{-1} cm^{-1}) and a shoulder at 660 nm (ε = ~1020 M^{-1} cm^{-1}), and is thus very different from the spectrum in borate buffer (Fig. 3). Addition of 2 eq of $AgBF_4$ to a CH_3CN solution of **2** (0.5 mM) results in substitution of the chloride ligand by a solvent molecule and the formation of $[Co^{II}(Py5OH)(CH_3CN)]^{2+}$ (**3**). This transformation can be followed by the disappearance of the ESI-MS peak for **2** at 541.1 ($[Co^{II}(Py5OH)(Cl)]^+$) and the emergence of a new peak at 548.5 (m/Z) ($[Co^{II}(Py5OH)(CH_3CN)]^+$-$H^+$) (Fig. S11). Ligand substitution from chloride to CH_3CN is also characterized by the disappearance of the distinct features in the UV-Vis spectrum of **2** at 588 nm and 685 nm and the appearance of a broad absorption at 505 nm (Fig. S2b). The sharp bands in the UV-vis spectrum of **2** in CH_3CN are thus markers for the presence of the chloride ligand at the Co^{II} centre.

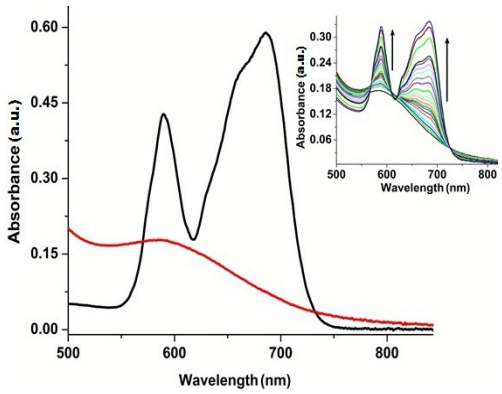

Fig. 3 UV-visible spectra of **2** (0.5 mM) in CH_3CN before (black) and after addition of 10 eq of *m*-CPBA (red). Inset: Recovery of **2** over a period of 2 h.

Upon addition of 10 eq *m*-CPBA to a CH_3CN solution of **2**, the sharp peaks at 588 and 685 nm disappear and a broad absorption with a maximum at 585 nm (ε ~ 360 M^{-1} cm^{-1}) emerges ($\mathbf{2^{ox}}$ red trace, Fig. 3). Within one minute after addition of *m*-CPBA, the initially obtained spectrum of $\mathbf{2^{ox}}$ changes and starts to revert back to the characteristic spectrum of **2** over a timescale of 2 h.

After the first minute, the spectral changes have clear isosbestic points at 570, 615 and 725 nm (Fig. 3, inset) which is indicative for the formation of **2** and the absence of any intermediate that would be stable on these timescales.[‡] ESI-MS investigations of the yellowish brown solution of $\mathbf{2^{ox}}$ at rapid positive detection mode shows a major peak at 522.1, which corresponds to $[Co^{III}(O)(Py5OH)]^+$ and an additional peak at 261.6 that can be assigned to $[Co^{III}(OH)(Py5OH)]^{2+}$ (Fig. S4c). Addition of 2 V% water to $\mathbf{2^{ox}}$ leads to faster regeneration of the spectral features associated with **2**, indicating that the active intermediate after addition of *m*-CPBA can utilize water as a substrate. Oxygen evolution induced by the addition of 10 eq of *m*-CPBA to CH_3CN solutions of **2** in the presence of 2 V% water was monitored by Clark electrode (Fig. S12a), and a quantitative amount of oxygen (TON ~5 mol O_2/mol **2**) could be detected. It is important to note that the chloride ligand is present at the Co^{II} centre also after catalytic turnover.

Addition of 10 eq of *m*-CPBA to a solution of the CH_3CN complex **3** results in the formation of a new species $\mathbf{3^{ox}}$ with broad absorption bands at 520 nm and 785 nm in its UV-VIS spectrum (Fig. S13a). ESI-MS spectra in rapid positive detection mode of $\mathbf{3^{ox}}$ show a distinct peak at 1024.8 (m/Z) (inset of Fig. S13b). This peak is assigned to an oxo-bridged dinuclear Co^{III} species $[(Py5OH)Co^{III}(O)Co^{III}(Py5OH)3H^+]$. A multi-step regeneration of **3** (absorbance at 505 nm) can be observed during 30 min after the addition of *m*-CPBA (Fig. S13b) producing at least one more species with absorption in the NIR region (900-1000 nm). A second addition of *m*-CPBA after 30 min again leads to the formation of $\mathbf{3^{ox}}$ but with lower concentration. Oxygen evolution induced by 10 eq of *m*-CPBA in the presence of 2V% water and *in situ* generated **3** (Fig. S12b) proceeds in much lower yield as compared to the analogous experiment with **2**, and only 1.5 mol O_2/mol **3** can be detected.

These experiments clearly show that the presence of the chloride ion in the primary coordination sphere of the Co centre is important for oxygen evolution induced by *m*-CPBA. In the presence of the chloride, the reaction proceeds smoothly and oxygen is evolved quantitatively. The chloride appears to be coordinated throughout the reaction as **2** is regenerated after catalytic turnover. In contrast, when the chloride is absent, a relatively stable bridged dinuclear species accumulates in the reaction mixture and can be detected during the oxygen evolution reaction (Fig. S13 and Scheme 2).

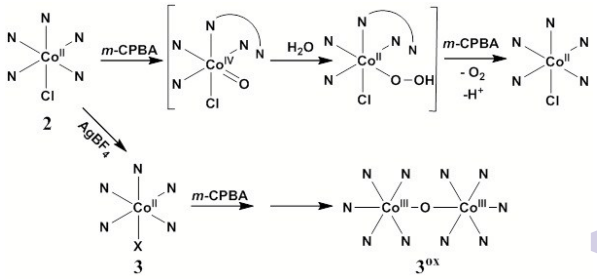

Scheme 2 Proposed pathways for oxidation of **2** and **3** using *m*-CPBA. X is a labile ligand, probably MeCN.

The presence of the chloride ligand throughout the catalytic cycle requires the temporary detachment of a pyridine ligand to liberate a coordination site for substrate binding. We suggest that one of the four equatorial pyridine arms detaches during catalysis and rebinds after turnover (Scheme 2). This type of adaptive ligand coordination is unusual, but has recently been proposed to explain the water oxidation activity of a dinuclear cobalt complex.[5d] A similar detachment of an equatorial pyridine to allow the coordination of an hydroxide ion has also been proposed by Crandell et al. in a theoretical study on the closely related Co(Py5) complex.[8] In comparison to Co(Py5) where the sixth coordination site is occupied by a water molecule, the higher donor strength of the chloride in **2** could energetically facilitate the detachment of one of the equatorial pyridine ligands.

Having established the importance of the chloride ligand for facile catalysis in CH_3CN, a similar investigation was conducted in water. Also in water, removal of the chloride in **2** can be achieved by the addition of $AgBF_4$, and followed by the evolution of a UV-Vis spectrum with an absorption maximum at 505 nm (Fig. S2a). This

spectrum is very similar to that of the corresponding species **3** in CH_3CN. Moreover, after the reaction of **2** with $AgBF_4$ in water the peak at 541.1 ($[Co^{II}(Py5OH)(Cl)]^+$ completely disappears in the mass spectrum of **2** (Fig. S14). It is thus clear that the chloride is substituted by a water molecule under these conditions, and the product is assigned to $[Co^{II}(Py5OH)(H_2O)](BF_4)_2$ (**4**).

Water oxidation activity for **4** was investigated using a freshly prepared solution of $[Ru^{III}(bpy)_3]^{3+}$ as chemical oxidant at pH 8 (borate buffer) with a Co to Ru^{III} ratio of 1:100 (Fig. S6a). Only 6.5 mol(O_2) mol(**4**)$^{-1}$ were evolved using **4** as catalyst, equivalent to ~25 % yield compared to the 60 % yield observed for **2**. The experiments thus indicate that the presence of the chloride ligand plays an important role for water oxidation also in aqueous solution. Mechanistically, this implies that a pyridine has to detach from the Co centre during the cause of the catalytic cycle to allow for substrate binding.

In conclusion, the efficiency of $[Co^{II}(Py5OH)Cl](BF_4)$ (**2**) for catalytic water oxidation and oxygen evolution has been investigated. DLS measurements and the regeneration of the characteristic UV-Vis spectrum of **2** after m-CPBA induced oxygen evolution confirm the molecular integrity of the catalyst during turnover. The importance of the chloride ligand as integral component of the catalyst has been established, and was found to prevent the formation of a dinuclear Co^{III}_2 species that impedes catalytic turnover in wet CH_3CN. With the chloride ligand present, complex **2** shows higher catalytic activity than *in situ* generated **3** and **4** that lack the chloride ligand. These observations together with ESI-MS measurements allow us to propose a mechanism for water oxidation catalysed by **2** where the chloride stays coordinated during catalysis and one of the pyridine arms detach from the first coordination sphere to enable substrate binding (Scheme 2).

We gratefully acknowledge Swedish Energy Agency, the Knut and Alice Wallenberg Foundation and the Swedish Research Council for funding. We would like to thank E. Zeglio for the help with the DLS experiments and Dr S. Maji for helpful discussions.

Notes and references

† The potential for catalytic water oxidation (E_{Wox}) was taken as the potential where the current was twice that of the first quasi-reversible oxidation. The overpotential for water oxidation is then defined as E_{Wox}–(1.23–(0.059·pH)).

‡ DLS measurements of **2** in MeCN treated with *m*-CPBA (1, 5 and 10 eq) show no nanoparticle formation and confirm the molecular integrity of **2** in presence of 10 eq of *m*-CPBA.

1 (a) B. Loll, J. Kern, W. Saenger, A. Zouni and J. Biesiadka, *Nature*, 2005, **438**, 1040–1044; (b) J. Yano and V. K. Yachandra, *Inorg. Chem.*, 2008, **47**, 1711; (c) J. P. McEvoy and G. W. Brudvig, *Chem. Rev.*, 2006, **106**, 4455; (d) T. R. Cook, D. K. Dogutan, S. Y. Reece, Y. Surendranath, T. S. Teets, and D. G. Nocera, *Chem. Rev.*, 2010, **110**, 6474–6502; (e) K. N. Ferreira, T. M. Iverson, K. Maghlaoui, J. Barber and S. Iwata, *Science*, 2004, **303**, 1831; (f) M. D. Kärkäs, O. Verho, E. V. Johnston and B. Åkermark, Chem. Rev., 2014, 114, 11863–12001.

2 S. W. Gersten, G. J. Samuels and T. J. Meyer, *J. Am. Chem. Soc.*, 1982, **104**, 4029–4030.

3 (a) J. F. Hull, D. Balcells, J. D. Blakemore, C. D. Incarvito, O. Eisenstein, G. W. Brudvig and R. H. Crabtree, *J. Am. Chem. Soc.*, 2009, **131**, 8730–8731; (b) Y. V. Geletii, Z. Q. Huang, Y. Hou, D. G. Musaev, T. Q. Lian and C. L. Hill, *J. Am. Chem. Soc.*, 2009, **131**, 7522–7523; (c) L. L. Duan, Y. H. Xu, P. Zhang, M. Wang and L. C. Sun, *Inorg. Chem.*, 2010, **49**, 209–215; (d) C. Sens, I. Romero, M. Rodriguez, A. Llobet, T. Parella and J. Benet–Buchholz, *J. Am. Chem. Soc.*, 2004, **126**, 7798–7799; (e) A. M. Angeles-Boza, M. Z. Ertem, B. R. Sarma, C. H. Ibanez, S. Maji, A. Llobet, Christopher J. Cramer and J. D. Roth, *Chem. Sci.*, 2014, 5, 1141–1152; (f) R. Zong and R. Thummel, *J. Am. Chem. Soc.*, 2005, **127**, 12802–12803; (g) S. Maji, I. López, F. Bozoglian, J. Benet-Buchholz and A. Llobet, *Inorg. Chem.*, 2013, **52**, 3591−3593; (h) A. Petronilho, M. Rahman, J. A. Woods, H. Al-Sayyed, H. Müller-Bunz, J. M. Don MacElroy and S. Bernhard, M. Albrecht, *Dalton Trans.*, 2012, **41**, 13074–13080; (i) L. Duan, F. Bozoglian, S. Mandal, B. Stewart, T. Privalov, A. Llobet, and L. Sun, *Nat. Chem.*, 2012, **4**, 418–423.

4 (a) D. J. Wasylenko, C. Ganesamoorthy, J. Borau-Garcia and C. P. Berlinguette, *Chem. Commun.*, 2011, **47**, 4249–4251; (b) D. Hong, J. Jung, J. Park, Y. Yamada, T. Suenobu, Y-M. Lee, W. Nam and S. Fukuzumi, *Energy Environ. Sci.*, 2012, **5**, 7604–7616; (c) H. Wang, Y. Lu, E. Mijangos and A. Thapper, *Chin. J. Chem.*, 2014, **32**, 467–473; (d) D. K. Dogutan, R. McGuire Jr., D. G. Nocera, *J. Am. Chem. Soc.*, 2011, **133**, 9178–9180; (e) C.-F. Leung, S.-M. Ng, C.-C. Ko, W.-L. Man, J. Wu, L. Chen and T.-C. Lau, *Energy Environ. Sci.*, 2012, **5**, 7903–7907; (f) Y. Tanaka, M. Annaka, K. Sakai, *Chem. Commun.*, 2012, **48**, 1653–1655; (g) D. J. Wasylenko, R. D. Palmer, E. Schott, C. P. Berlinguette, *Chem. Commun.*, 2012, **48**, 2107–2109; (h) E. Pizzolato, M. Natali, B. Posocco, A. Montellano Lopez, F. Bazzan, M. Di Valentin, P. Galloni, V. Conte, M. Bonchio, F. Scandola, A. Sartorel, *Chem. Commun.*, 2013, **49**, 9941–9943; (i) T. Nakazono, A. R. Parent, K. Sakai, *Chem. Commun.*, 2013, **49**, 6325–6327; (j) I. Siewert and J. Gałezowska, *Chem. Eur. J.*, 2015, **21**, 2780–2784.

5 (a) H.-Y. Wang, E. Mijangos, S. Ott, and A. Thapper, *Angew. Chem. Int. Ed.*, 2014, **53**, 14499–14502; (b) J. Luo , N. P. Rath and L. M. Mirica, *Inorg. Chem.*, 2011, **50**, 6152–6157; (c) M. L. Rigsby, S. Mandal, W. Nam, L. C. Spencer, A. Llobet, S. Stahl, *Chem. Sci.*, 2012, **3**, 3058–3062; (d) M. Chen, S.-M. Ng, S.-M. Yiu, K.-C. Lau, R. J. Zeng and T.-C. Lau, *Chem. Commun.*, 2014, **50**, 14956-14959.

6 (a) S. Berardi, G. La Ganga, M. Natali, I. Bazzan, F. Puntoriero, A. Sartorel, F. Scandola, S. Campagna, M. Bonchio, *J. Am. Chem. Soc.*, 2012, **134**, 11104–11107; (b) N. S. McCool, D. M. Robinson, J. E. Sheats, G. C. Dismukes, *J. Am. Chem. Soc.*, 2011, **133**, 11446–11449; (c) F. Evangelisti, R. Guttinger, R. More, S. Luber, G. R. Patzke, *J. Am. Chem. Soc.*, 2013, **135**, 18734–18737.

7 (a) Q. Yin, J. M. Tan, C. Besson, Y. V. Geletii, D. G. Musaev, A. E. Kuznetsov, Z. Luo, K. I. Hardcastle, C. L. Hill, *Science*, 2010, **328**, 342–345; (b) N. Planas, L. Vigara, C. Cady, P. Miró, J. Huang, L. Hammarström, S. Styring, N. Leidel, H. Dau, M. Haumann, L. Gagliardi, C. J. Cramer, A. Llobet, *Inorg. Chem.*, 2011, **50**, 11134–11142.

8 D. W. Crandell, S. Ghosh, C. P. Berlinguette and M.-H. Baik, *ChemSusChem*., 2015, **8**, 844-852.

9 R. T. Jonas and T. D. P. Stack, *J. Am. Chem. Soc.*, 1997, **119**, 8566–8567.

10 Y. V. Geletii, B. Botar, P. K. Gerler, D. A. Hillesheim, D. G. Musaev, C. L. Hill, *Angew. Chem. Int. Ed.*, 2008, **47**, 3896–3899.

11 P. J. Cameron, L. M. Peter, S. M. Zakeeruddin and M. Grätzel, *Coord. Chem. Rev.*, 2004, **248**, 1447–1453.